

A Search for Vector Diquarks at the CERN LHC

E. Arik^a, O. Çakır^b, S. A. Çetin^a and S. Sultansoy^{c,d}

^a *Bogazici University, Faculty of Sciences, Department of Physics,
80815, Bebek, Istanbul, Turkey*

^b *Ankara University, Faculty of Sciences, Department of Physics,
06100 Tandogan, Ankara, Turkey*

^c *Gazi University, Faculty of Arts and Sciences, Department of Physics,
06500, Teknikokullar, Ankara, Turkey*

^d *Azerbaijan Academy of Sciences, Institute of Physics,
H. Cavid av., 33, Baku, Azerbaijan*

Resonant production of the first generation vector diquarks at the CERN Large Hadron Collider (LHC) have been investigated. It is shown that the LHC will be able to discover vector diquarks with masses up to 9 TeV if coupling $\alpha_D = 0.1$.

I. INTRODUCTION

The existence of at least three fermion families naturally leads to the hypothesis that they are made up of more fundamental constituents frequently called preons [1]. Today, the compositeness should be considered as a candidate for beyond the standard model (BSM) physics on the same footing as SUSY. Moreover, some assumptions made in order to get rid of huge number of free parameters in three family MSSM have natural explanation (see [2] and references therein) in the framework of preonic models. These models predict a rich spectrum of new particles with unusual quantum numbers at high energies such as excited quarks and leptons, diquarks, dileptons, leptoquarks, leptogluons, sextet quarks, octet bosons etc. In preonic models, diquarks are as natural as leptoquarks [3]. They are colored objects having integer-spin and baryon number $|B| = 2/3$. Diquarks are also predicted in the framework of superstring-inspired E_6 models [4].

Recent collider limits on the diquark masses come from Tevatron data which exclude the region $290 < M_D < 420$ GeV (for E_6 diquarks) [5]. Diquark production at e^+e^- colliders, ep colliders and $p\bar{p}$ colliders have been analyzed in [6], [7] and [8] respectively. Recently, the resonance production of scalar diquarks at CERN LHC has been studied in [9].

In this work, the sensitivity of LHC to composite vector diquark production is estimated. In section II, interaction lagrangian and quantum numbers of diquarks are discussed. Decay width and production cross section of a vector diquark at the CERN LHC are considered in section III. Then, in section IV, vector diquark signal and corresponding backgrounds are analyzed. Finally, in section V we give some conclusions and remarks.

II. INTERACTION LAGRANGIAN AND CLASSIFICATION

A model independent, baryon number conserving, most general $SU(3)_C \times SU(2)_W \times U(1)_Y$ invariant effective lagrangian for diquarks has the form

$$\begin{aligned} L_{|B|=0} = & f_{1L}\bar{q}_L\gamma^\mu q_L D_{1\mu}^c + (f_{1R}\bar{d}_R\gamma^\mu d_R + f'_{1R}\bar{u}_R\gamma^\mu u_R)D_{1\mu}^c \\ & + \tilde{f}_{1R}\bar{u}_R\gamma^\mu d_R \tilde{D}_{1\mu}^c + f_{3L}\bar{q}_L\tau\gamma^\mu q_L \cdot \mathbf{D}_{3\mu}^c \\ & + f_2\bar{q}_L i\tau_2 u_R D_2^c + \tilde{f}_2\bar{q}_L i\tau_2 d_R \tilde{D}_2^c + \text{H.c.} \end{aligned} \quad (1)$$

$$\begin{aligned} L_{|B|=2/3} = & (g_{1L}\bar{q}_L^c i\tau_2 q_L + g_{1R}\bar{u}_R^c d_R)D_1^c + \tilde{g}_{1R}\bar{d}_R^c d_R \tilde{D}_1^c \\ & + \tilde{g}'_{1R}\bar{u}_R^c u_R \tilde{D}_1^c + g_{3L}\bar{q}_L^c i\tau_2 \tau q_L \cdot \mathbf{D}_3^c \\ & + g_2\bar{q}_L^c \gamma^\mu d_R D_{2\mu}^c + \tilde{g}_2\bar{q}_L^c \gamma^\mu u_R \tilde{D}_{2\mu}^c + \text{H.c.} \end{aligned} \quad (2)$$

The $B = 0$ diquarks are familiar fields, as they resemble the electroweak gauge vectors, and the neutral and charged Higgs scalars. Here, we consider only the $B = 2/3$ diquarks. An effective lagrangian for F=2 scalar and vector diquarks is given in Ref. [9]. In Eq. (2), $q_L = (u_L, d_L)$ and $q^c = C\bar{q}^T$ ($\bar{q}^c = -q^T C^{-1}$). For the sake of simplicity, color and generation indices are omitted. Scalar diquarks $D_1, \tilde{D}_1, \tilde{D}'_1$ are $SU(2)_W$ singlets and \tilde{D}_3 is $SU(2)_W$ triplet.

Vector diquarks D_2 and \tilde{D}_2 are $SU(2)_W$ doublets. Diquarks may transform as anti-triplet or sextet under $SU(3)_C$. At this stage, we assume that each SM generation has its own diquarks and couplings in order to avoid flavour changing neutral currents. Furthermore, the members of a given multiplet are assumed to be the mass degenerated.

Lagrangian (2) can be rewritten in the following more transparent form:

$$L = L_S + L_V \quad (3)$$

$$L_S = [g_{1L} (\bar{u}^c P_L d - \bar{d}^c P_L u) + g_{1R} \bar{u}^c P_R d] D_1 + \tilde{g}_{1R} \bar{d}^c P_R d \tilde{D}_1 + \tilde{g}'_{1R} \bar{u}^c P_R u \tilde{D}'_1 + \sqrt{2} g_{3L} \bar{u}^c P_L u D_3^+ - \sqrt{2} g_{3L} \bar{d}^c P_L d D_3^- - g_{3L} (\bar{u}^c P_L d + \bar{d}^c P_L u) D_3^0 + \text{H.c.} \quad (4)$$

$$L_V = g_2 \bar{u}^c \gamma^\mu P_R d D_{2\mu}^{1c} + g_2 \bar{d}^c \gamma^\mu P_R d D_{2\mu}^{2c} + \tilde{g}_2 \bar{u}^c \gamma^\mu P_R u \tilde{D}_{2\mu}^{1c} + \tilde{g}_2 \bar{d}^c \gamma^\mu P_R u \tilde{D}_{2\mu}^{2c} + \text{H.c.} \quad (5)$$

where $P_L = (1 - \gamma_5)/2$ and $P_R = (1 + \gamma_5)/2$. A general classification of the first generation, color $\bar{\mathbf{3}}$ diquarks is shown in Table I.

III. DECAY WIDTH AND PRODUCTION CROSS SECTION

For the present analysis, we consider the color $\bar{\mathbf{3}}$ vector diquark D_2 which couples to ud -pair as described by the effective lagrangian (2). The decay width Γ_D , derived from the same lagrangian, is

$$\Gamma_D = C_F \frac{g_2^2 M_D}{24\pi} \quad (6)$$

where C_F is the color factor for triplet representation and M_D is the mass of vector diquark. We will use the definition $g_2^2 = 4\pi\alpha_D$ for numerical results

$$\Gamma_D = C_F \frac{\alpha_D M_D}{6} \simeq 17 \text{ GeV} \left(\frac{C_F M_D}{1 \text{ TeV}} \right) \quad \text{for } \alpha_D = 0.1 \quad (7)$$

In the narrow width approximation ($\Gamma/M < 0.1$), the cross section of the s-channel diquark resonance production can be obtained as

$$\sigma(pp \rightarrow D_2 X) = \sum_{ab} \frac{C_F^2 \alpha_D \pi^2}{s} \int_{M_D^2/s}^1 \frac{dx}{x} f_a(x, \hat{s}) f_b\left(\frac{M_D^2}{sx}, \hat{s}\right) \quad (8)$$

where $\hat{s} = x_a x_b s$, f_a and f_b are quark distribution functions of each proton. In Fig. 1, using the CTEQ5L quark distribution functions [10], the cross section versus diquark mass is plotted for LHC energy ($\sqrt{s} = 14 \text{ TeV}$) with $\alpha_D = 0.1$.

IV. SIGNAL AND BACKGROUND

D_2 -type diquark s-channel resonance will be formed via the subprocess $q_i q_j \rightarrow D_2$. Therefore, the signal will contain two hard jets in the final state. Considering only the interference with the t-channel gluon exchange, the following differential cross section is obtained:

$$\begin{aligned} \frac{d\hat{\sigma}}{d\hat{t}}(q_i q_j \rightarrow q_i q_j) &= C_F^2 \pi \left[\frac{\alpha_D^2 (\hat{s} + \hat{t})^2}{\hat{s}^2 [(\hat{s} - M_D^2)^2 + M_D^2 \Gamma_D^2]} \right. \\ &\quad \left. + \frac{2\alpha_s^2 (2\hat{s}^2 + \hat{t}^2 + 2\hat{s}\hat{t})}{\hat{s}^2 \hat{t}^2} - \frac{2\alpha_D \alpha_s}{\hat{t}} \frac{(\hat{s} + \hat{t})^2 (\hat{s} - M_D^2)}{\hat{s}^2 [(\hat{s} - M_D^2)^2 + M_D^2 \Gamma_D^2]} \right] . \quad (9) \end{aligned}$$

At LHC energy, major QCD processes contributing to two jet (jj) final states and their integrated cross sections are given in Table II. The values in Table II have been generated by PYTHIA 6.1 [11] at parton level with various p_T cuts. It is clear that higher p_T cuts reduce the background cross sections significantly. These p_T cuts can be translated into the rapidity cuts via the relation between the p_T of a jet and the rapidity y given by $p_T = M_{jj}/2 \cosh y$.

The cross section for the diquark mentioned above as a function of the dijet invariant mass M_{jj} with the rapidity cut $|y_{1,2}| \leq Y$, where y_1 and y_2 are rapidities of the massless final quarks, is given by

$$\begin{aligned}
\frac{d\sigma}{dM_{jj}} &= \frac{M_{jj}^3}{2s} \int_{-Y}^Y dy_2 \int_{y_1^{\min}}^{y_1^{\max}} dy_1 \frac{1}{\cosh^2 y^*} \\
&\times [f_{u/A}(x_u, Q^2) f_{d/B}(x_d, Q^2) \frac{d\hat{\sigma}}{d\hat{t}}(\hat{s}, \hat{t}, \hat{u}) \\
&+ f_{d/A}(x_d, Q^2) f_{u/B}(x_u, Q^2) \frac{d\hat{\sigma}}{d\hat{t}}(\hat{s}, \hat{u}, \hat{t})]
\end{aligned} \tag{10}$$

with

$$\begin{aligned}
y^* &= (y_1 - y_2)/2, & y^b &= (y_1 + y_2)/2 \\
x_u &= \sqrt{\tau} e^{y^b}, & x_d &= \sqrt{\tau} e^{-y^b} \\
\hat{s} &= x_u x_d s, & \hat{t} &= -x_u p_T \sqrt{s} e^{-y_1}, & \hat{u} &= -x_d p_T \sqrt{s} e^{y_1} \\
y_1^{\min} &= \max(-Y, \log \tau - y_2), & y_1^{\max} &= \min(Y, -\log \tau - y_2), & \tau &= M_{jj}^2/s \quad .
\end{aligned}$$

Fig. 2 shows jet-jet invariant mass distribution for the process $pp \rightarrow D_2 \rightarrow jjX$ together with the estimates of the QCD backgrounds at LHC. For comparison, signal peaks for vector diquark masses $M_D = 2, 4, 6, 8$ TeV and $\alpha_D = 0.1$ are superimposed on the background distribution.

We have estimated background events for an integrated LHC luminosity of 10^5 pb^{-1} taking into account, as an example, the energy resolution of ATLAS hadronic calorimeter [12]:

$$\frac{\delta E}{E} = \frac{50\%}{\sqrt{E}} + 3\% \tag{11}$$

for jets with $|y| < 3$. The mass resolution can be expressed as [9]

$$\frac{\Delta M}{M} \approx \frac{\delta E}{\sqrt{2}E} \quad . \tag{12}$$

We have chosen ΔM as the mass window centered at M_D for signal and background estimations. Here, we take the energy of a jet $E \approx M_D/2$. For signal estimation the mass window ΔM is taken to be $2\Gamma_D$. This corresponds to the 95% CL for statistical acceptance. The cross sections are calculated by using the formula

$$\sigma = \int_{M_D - \Delta M}^{M_D + \Delta M} dM_{jj} \left(\frac{d\sigma}{dM_{jj}} \right) \tag{13}$$

Number of signal (S) and background (B) events, and the corresponding significances with $\alpha_D = 0.1$ are tabulated in Table III. Evidently, tighter cut on the rapidity y improves the significance considerably. In Table IV, we present the achievable M_D limits for different values of α_D . As discovery criteria, we adopt $S/\sqrt{B} \geq 5$ and $S \geq 25$.

In Fig. 3, the attainable mass limits are presented in the plane (α_D, M_D) . The LHC potential for the discovery of D_2 is clearly demonstrated in Fig. 4 where minimum integrated luminosities, needed to satisfy the adopted criteria, are plotted as a function of M_D for various α_D values.

V. CONCLUSION

The resonance production of vector diquarks at LHC has large cross section. With reasonable cuts, it may be possible to cover mass ranges up to 9 TeV for coupling $\alpha_D = 0.1$. For smaller couplings as $\alpha_D = 5 \times 10^{-4}$, it is still possible to probe diquarks up to the mass of 4 TeV at an integrated luminosity $L = 10^2 \text{ fb}^{-1}$.

VI. REFERENCES

- [1] H. Terazawa, Phys. Rev. 22 (1980) 184; H. Harari, Phys. Rep. 104 (1984) 159; D'Souza and Kalman, Preons, World Scientific Publishing, (1992).
- [2] S. Sultansoy, hep-ph/0003269 (2000).
- [3] J. Wudka, Phys. Lett. B167 (1986) 337.
- [4] J.L. Hewett and T.G. Rizzo, Phys. Rep. 183 (1989) 193.
- [5] F. Abe *et al.*, CDF Collaboration, Phys. Rev. Lett. 77 (1996) 5336; B. Abbott *et al.*, D0 Collaboration, Phys. Rev. Lett. 80 (1998) 666.
- [6] D. Schaile and P.M. Zerwas: Proceedings of the Workshop on Physics at Future Accelerators, CERN Yellow Report 87-07, Vol. II, p.251 (1987).
- [7] T.G. Rizzo, Z. Phys. C43 (1989) 223.
- [8] V.D. Angelopoulos *et al.*, Nucl. Phys. B292, 59 (1987).
- [9] S. Atağ, O. Çakır, and S. Sultansoy, Phys. Rev. D59, 015008 (1998).
- [10] CTEQ Collaboration, H.L. Lai *et al.*, Eur.Phys. J. **C12** (2000) 375.
- [11] Torbjörn Sjöstrand *et al.* hep-ph/0010017 (2000).
- [12] ATLAS Collaboration, ATLAS TDR 14, CERN/LHCC 99-14 (1999).

TABLE I. Quantum numbers of the first generation, color $\bar{3}$ diquarks described by the effective lagrangian in the text according to $SU(3)_C \times SU(2)_W \times U(1)_Y$ invariance. $Q_{em} = I_3 + Y/2$

Scalar Diquarks	$SU(3)_C$	$SU(2)_W$	$U(1)_Y$	Q	Couplings
D_1	3^*	1	2/3	1/3	$u_L d_L(g_{1L}), u_R d_R(g_{1R})$
\bar{D}_1	3^*	1	-4/3	2/3	$d_R d_R(\tilde{g}_{1R})$
\bar{D}'_1	3^*	1	8/3	4/3	$u_R u_R(\tilde{g}'_{1R})$
D_3	3^*	3	2/3	$\begin{pmatrix} 4/3 \\ 1/3 \\ -2/3 \end{pmatrix}$	$\begin{pmatrix} u_L u_L(\sqrt{2}g_{3L}) \\ u_L d_L(-g_{3L}) \\ d_L d_L(-\sqrt{2}g_{3L}) \end{pmatrix}$
Vector Diquarks					
$D_{2\mu}$	3^*	2	-1/3	$\begin{pmatrix} 1/3 \\ -2/3 \end{pmatrix}$	$\begin{pmatrix} d_R u_L(g_2) \\ d_R d_L(-g_2) \end{pmatrix}$
$\bar{D}_{2\mu}$	3^*	2	5/3	$\begin{pmatrix} 4/3 \\ 1/3 \end{pmatrix}$	$\begin{pmatrix} u_R u_L(\tilde{g}_2) \\ u_R d_L(-\tilde{g}_2) \end{pmatrix}$

TABLE II. Cross sections (pb) for QCD backgrounds contributing to j-j final states at parton level generated by PYTHIA 6.1 with various cuts.

Process	$p_T > 100$ GeV	$p_T > 500$ GeV	$p_T > 1000$ GeV	$p_T > 1500$ GeV	$p_T > 2000$ GeV
$gg \rightarrow gg$	6.3×10^9	2.0×10^2	2.3×10^0	8.6×10^{-2}	5.7×10^{-3}
$q_i g \rightarrow q_i g$	6.4×10^5	4.8×10^2	1.0×10^1	6.4×10^{-1}	5.7×10^{-2}
$q_i q_j \rightarrow q_i q_j$	1.0×10^5	1.8×10^2	6.7×10^0	6.3×10^{-1}	8.8×10^{-2}
$gg \rightarrow q_k \bar{q}_k$	2.4×10^4	9.8×10^0	1.0×10^{-1}	4.9×10^{-3}	2.9×10^{-4}
$q_i \bar{q}_i \rightarrow q_k \bar{q}_k$	1.6×10^3	2.8×10^0	1.3×10^{-1}	9.0×10^{-3}	1.1×10^{-3}
$q_i \bar{q}_i \rightarrow gg$	1.5×10^3	2.5×10^0	6.7×10^{-2}	8.1×10^{-3}	8.5×10^{-4}
Total	1.4×10^6	8.8×10^2	1.9×10^1	1.4×10^0	1.5×10^{-1}

TABLE III. Observability of the vector diquark D_2 with $\alpha_D = 0.1$ at LHC for $L_{int} = 10^5 \text{pb}^{-1}$.

M_D (TeV)	1	2	3	4	5	6	7	8	9
$ y < 2$									
S	7.7×10^7	6.6×10^6	1.1×10^6	2.4×10^5	5.0×10^4	9.9×10^3	1.7×10^3	2.5×10^2	2.7×10^1
B	2.8×10^8	5.6×10^6	4.2×10^5	5.4×10^4	8.4×10^3	1.4×10^3	2.2×10^2	3.0×10^1	3.1×10^0
S/\sqrt{B}	4585	2787	1768	1027	545	266	118	46	16
$ y < 1$									
S	2.6×10^7	2.8×10^6	5.8×10^5	1.3×10^5	2.9×10^4	6.1×10^3	1.1×10^3	1.6×10^2	1.8×10^1
B	2.5×10^7	5.2×10^5	4.0×10^4	5.0×10^3	7.9×10^2	1.3×10^2	2.1×10^1	2.8×10^0	3.0×10^{-1}
S/\sqrt{B}	5213	3946	2889	1842	1044	534	245	99	34

TABLE IV. Achievable diquark mass limits for different diquark-quark-quark couplings in the framework of discovery criteria given in the text. $|y| < 2$.

α_D	M_D (TeV)	S	B	S/\sqrt{B}
0.1	9	27	3.1	16.0
0.01	8	25	30	4.6
0.001	5	500	8400	5.4
0.0005	4	1200	540006	5.1

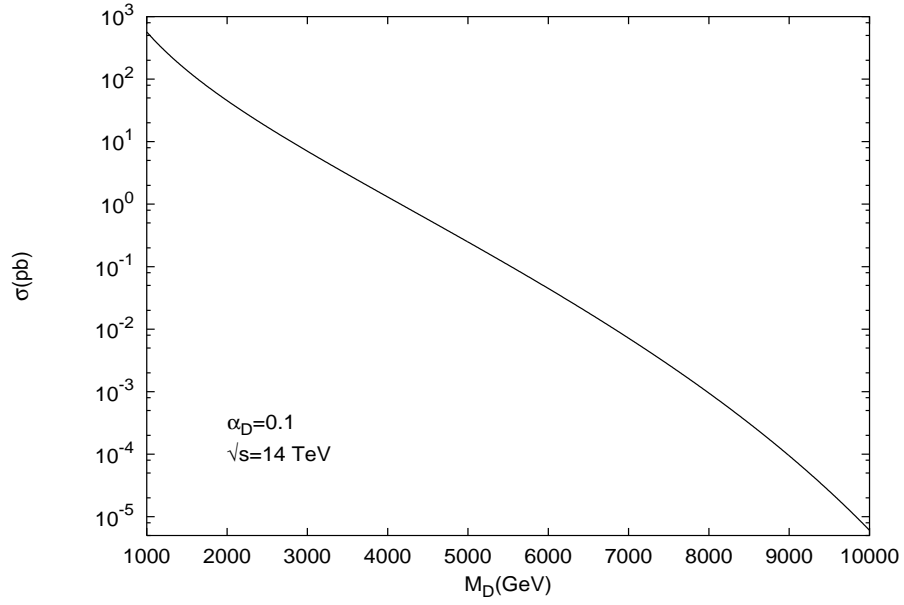


FIG. 1. Integrated cross section versus diquark mass for coupling strength $\alpha_D = 0.1$.

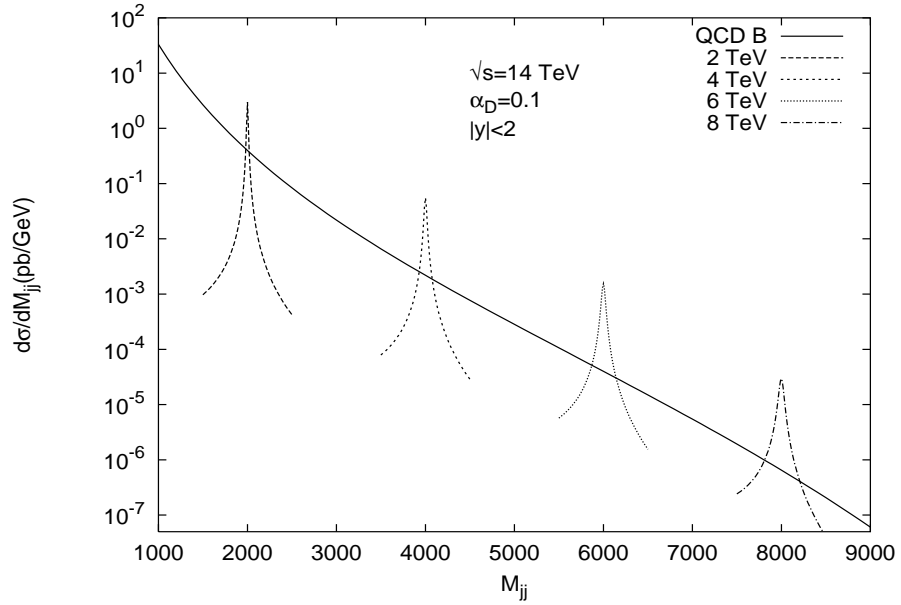


FIG. 2. Dijet invariant mass distribution for $M_D = 2, 4, 6, 8$ TeV superimposed over the QCD background.

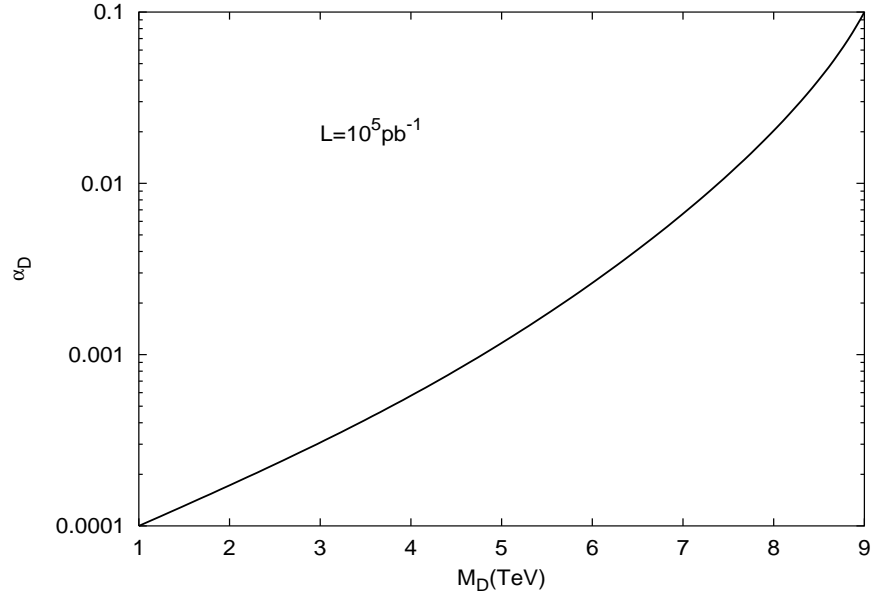


FIG. 3. Attainable limits for diquarks in α_D - M_D plane.

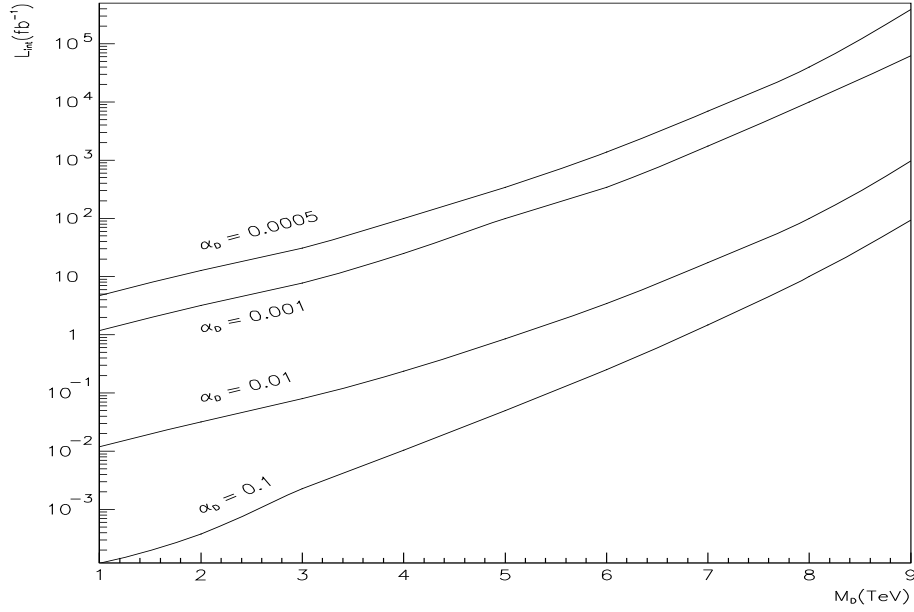


FIG. 4. The minimum integrated luminosities, needed to satisfy the adopted discovery criteria, as a function of M_D for various α_D values.